
Proceedings Paper:
Daskalakis, E, Jha, A orcid.org/0000-0003-3150-5645, Scott, A et al. (1 more author) (2022) Phase and Microstructural Analysis of In-Situ Derived Alumina-TiB2 Composites. In: TMS 2022 151st Annual Meeting & Exhibition Supplemental Proceedings. TMS 2022 151st Annual Meeting & Exhibition, 27 Feb - 03 Mar 2022, Anaheim, California, USA. Springer, Cham , pp. 49-59. ISBN 9783030923808

https://doi.org/10.1007/978-3-030-92381-5_6

Phase and Microstructural Analysis of In-Situ Derived Alumina-TiB_2 Composites

Corresponding Author: Evangelos Daskalakis[a] Evangelos.Daskalakis@outlook.com,

Other Authors: Animesh Jha[a] A.Jha@leeds.ac.uk, Andrew Scott[a] A.J.Scott@leeds.ac.uk, Ali Hassanpour[a] A.Hassanpour@leeds.ac.uk

[a] School of Chemical and Process Engineering, University of Leeds, Leeds LS2 9JT, UK

The paper focusses on the phase and microstructural evolution in ceramic composite based on alumina and titanium diboride, in which the precursor materials are aluminium mixed with TiO_2 and B_2O_3. The highly exothermic, self-sustaining, aluminothermic reaction ($\frac{10}{3}Al + TiO_2 + B_2O_3 = \frac{5}{3}Al_2O_3 + TiB_2$, $\Delta H = 2{,}710\frac{kJ}{mol}$) occurs in the absence of oxygen. Eventually, triggering the self-sustaining reaction on compacts formed from a ball-milled derived mixture, consisted of Al particles coated with TiO_2 and B_2O_3 nano-particles, resulted in the spontaneous formation of a ceramic phase mixture consisted of alumina particles coated with TiB_2 and Ti_2O_3 nano-particles. The highly exothermic character of the reaction enabled the sintering of the coated Al_2O_3 particles into a dense unique microstructure.

Keywords: Self -Sustaining Reaction, Ceramic Composites, Al_2O_3 – TiB_2

Introduction

Ceramic matrix composites exhibit advanced mechanical, thermal and electrical properties compared to the base matrices they derive from. The Al_2O_3/TiB_2 ceramic composite, is a structurally and thermodynamically compatible structure, which displays high hardness, stiffness, wear resistance, strength, fracture toughness and sinter-ability (1, 2).

As already known in the literature, alumina is an insulator and has low thermal expansion coefficient, good thermal stability but poor thermal shock resistance, while it is highly resistant to oxidation (3). By contrast titanium diboride exhibits much higher heat and electrical conductivity (4). Compared to alumina, TiB_2 is a much better conductor of heat and electricity because of the Ti-Ti bonding along the 0001 plane of hexagonal structure. The Ti-Ti layer imparts metallic bonding whereas the B-B layer provides covalent bonding. In the ABAB.. stacking of Ti-Ti and B-B layers, the mixed bonding is manifested along the c-axis of the hexagonal structure (5).

Since alumina and TiB_2 have closed packed hexagonal structure, their thermal, physical and mechanical properties are anisotropic (5). Therefore the properties compared in Table 1, display minimum and maximum values (3). Alumina has a higher expansion coefficient value compared to titanium diboride, Table 1, thus alumina is the matrix, while titanium diboride is the dispersion phase of the composite (2, 6, 7). This composite can find applications in impact-resistance armours, mechanical seals, aerospace, in wear resistance coating in cutting tools, crucibles and cathode material (8-11).

Table 1. Thermal, physical and mechanical properties of Al_2O_3 and TiB_2 (3, 12-14).

Properties	**Al_2O_3**	**TiB_2**
Density (g/cm^3)	3.95	4.52
Hardness (GPa)	5.5 – 22	25 – 35
Fracture Toughness (MPa/m^2)	3.3 – 5	6 – 8
Tensile Strength (MPa)	69 – 665	338 – 373
Shear Strength (GPa)	88 – 165	182 – 191
Expansion coefficient (10^{-6}/K)	7.8	7
Thermal Conductivity (W/mK)	12 – 38.5	25 – 90
Electrical conductivity (S/cm)	10^{-11}	10^5

The composite will be manufactured in situ, from a highly exothermic self-sustaining reaction due to its energy and cost efficiency, high products purity and advanced dispersion of secondary phase (2, 6-11). The alumina-thermic reaction of Equation 1, is thermodynamically favoured at room temperature, since the Gibbs free energy is negative, however reaction kinetics at room temperature are very slow and additional energy is required to trigger the overall reaction (6, 15-26).

Different reactant combinations are present in literature (2, 8, 9, 11, 27-48), however the oxides of boron and titanium decrease manufacturing cost, as the pure forms of Ti and B are 10 times and 100 times more expensive than TiO_2 and B_2O_3 respectively.

$$\frac{10}{3}\ Al + TiO_2 + B_2O_3 = \frac{5}{3}\ Al_2O_3 + TiB_2,\quad \Delta H = 2,710\ (\frac{kJ}{mol}) \qquad \text{Equation 1}$$

The adiabatic temperature of the reaction is 2,700 K, calculated by the generalised form of adiabatic temperature, given by equation (2) (6, 17, 18, 22-26, 49, 50). Where, a, b are two different solid phases, Tm is the melting point of second phase, Tad the adiabatic temperature and Cp is the heat capacity. Thermal analysis data of the reaction is displayed in table 4 (28).

$$\Delta H_{f,298} = \int_{To}^{Tt} Cp(a)dT + \Delta H_t + \int_{Tt}^{Tm} Cp\,(b)dT + v\Delta H_m + \int_{T_m}^{T_{ad}} Cp(liquid)dT \qquad \text{Equation 2}$$

Milling is a pre-processing technique of ceramic composites, leading to polymorphic transformation of the powder mixture. It aims in the reduction of the particles size, increase of the surface area and the delivery of a final mixture with specific particle size distribution. Size reduction is a result of fracture and wear, as a function of frequency of stress application and magnitude of stress (51, 52).

Powder pre-processing is feasible through different techniques, which follow mechanical, atomisation, aerosol, physical, chemical and plasma routes. Mechanical routes of processing metal and ceramic powders, include the sole use or combination of impaction, attrition, shear and compression. Powders subjected to these forces, undergo fracture, cold-welding and polymorphic transformation (52).

Materials and Methods

Stoichiometric powder mixture of (0.375) Al – (0.334) TiO_2 – (0.291) B_2O_3, is ball milled for 1 hour, split in two 30 minutes parts, with a 10 minute cooling interval, at 30 Hz. Milling takes place in an iron vessel, with an alumina impact ball, while the powder to ball weight ratio is 0.55. Then compacts with mass of 0.5 g are formed from cold pressing the as-milled mixture at 248 MPa.

Thermal analysis of the Al-TiO_2-B_2O_3 powder mixture, takes place with a Perkins Elmer Simultaneous Thermal Analyser (STA 6000), in argon environment. The maximum temperature is set at 1400 ^oC, while the heating rate is 20 ^oC per minute.

A tube furnace is used for the compacts' sintering, in argon atmosphere, with flowrate 2 L/min. Characterisation of sintered samples' is completed with X-Ray diffraction (XRD), scanning electron microscopy (SEM) and energy dispersive X-Ray spectroscopy (EDS).

For XRD, a Burker D8 Advance with monochromatic CuKα radiation (λ=0.154 nm) and a 2θ range of 10–90°, is used, for phases identification. Using Scherrer's equation, the average crystallite size of reactants and product phases is feasible, by calculating the area at FWHM, under the 100% peak of each of the phases, utilising equation $(\text{nm}) = (0.9\lambda)/(\text{B}\cos\theta)$ where B is the full width half maximum (in radians) of the XRD peak at angle 2θ and λ is the X-ray wavelength.

For SEM-EDS, a Hitachi SU8230 scanning electron microscope at 2-20 kV in backscattered and secondary electrons imaging modes was used. Samples were loaded on SEM metal stubs, carbon paint created a conductive path and along with carbon coating prevented sample's charging.

Results and Discussion

Milling of the stoichiometric powder mixture, resulted in particles' size reduction. X-Ray diffraction displays reduction in the peaks' intensity of the milled samples, as a result of particles' size reduction, Figure 1. Similar results are reported in literature (27-31, 53).

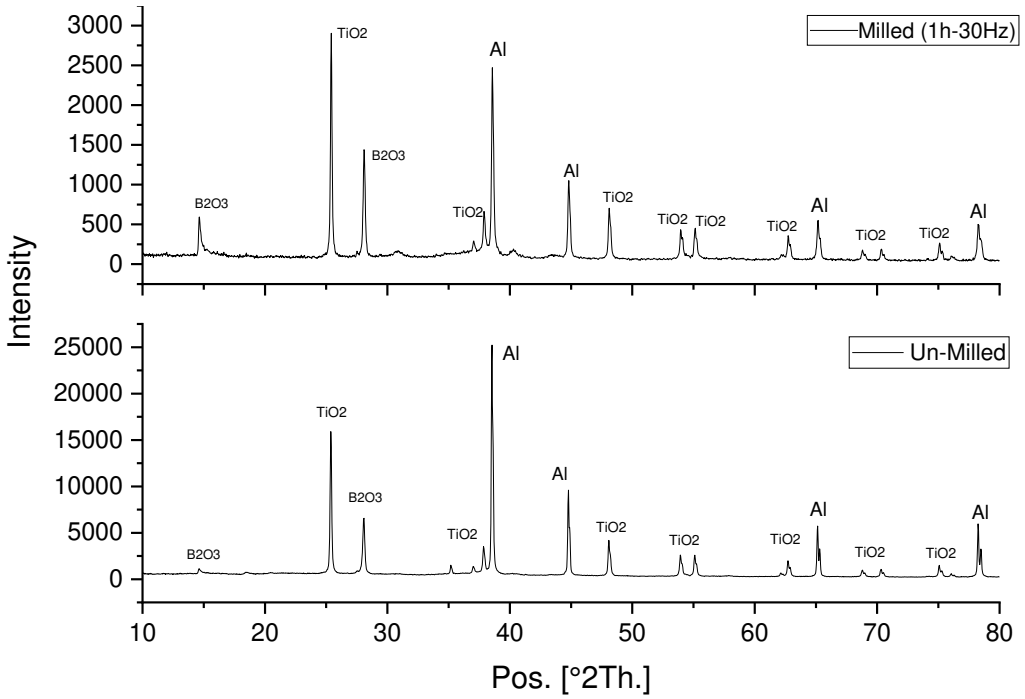

Figure 1. Phases identification of a) Milled. b) Un-milled powder mixtures, using X-Ray Diffraction with monochromatic CuKα radiation (λ=0.154 nm) and a 2θ range of 10–90°.

It is observed, that hard TiO_2 and B_2O_3 particles are being shattered, eventually coating the ductile Al particles, Figure 2, as seen in literature (27-31, 53). Aluminium particles have sizes of approximately 200 microns, while TiO_2 and B_2O_3 particle sizes range from 10 - 600 nm. From Scherrer's equation, crystallite sizes of reactants and products are calculated in Table 2. Crystallite sizes of TiO_2 and B_2O_3 oxides are smaller compared to the ones of ductile aluminium. Eventually the crystallite sizes of TiB_2 and Ti_2O_3, deriving from the smaller sized oxides, are smaller than alumina's.

Table 2. Crystal systems, cell volumes and crystallite sizes of reactants and products.

Milled 1h – 30Hz	Compound	**Al**	**TiO_2**	**B_2O_3**
	Crystal System	Cubic	Tetragonal	Cubic
	Cell Volume (10^6 pm^3)	66	136.03	1016
	Crystallite size(nm)	55.69	49.19	26.79
Sintered 1000 C	Compound	**Al_2O_3**	**TiB_2**	**Ti_2O_3**
	Crystal System	Rhombohedral	Hexagonal	Rhombohedral
	Cell Volume (10^6 pm^3)	254.7	25.63	312.4
	Crystallite size (nm)	53	47	33

Crystallite sizes of alumina and titanium diboride, deriving from in situ planetary ball milling, in literature, are shown in Table 3. The time required for the triggering of the reaction ranged between 1.5 – 60 h, as a result of the difference in energy input during milling, Table 3 (27-30). In the cases where planetary ball milling continued after the reaction completion, resulted in alumina displaying relatively lower crystallite size, compared to the cases where milling stopped right after reaction completion (28, 29). Crystallite sizes of alumina and titanium diboride calculated in Table 2, match the ones of literature, for mixtures where milling ceased right after reaction's completion.

Table 3. Crystallite sizes of alumina and titanium diboride.

Name	Final Crystal size (nm)	Milling Time (h)	Reaction Time (h)
Mohammad Sharifi et al.(27)	50 nm Al_2O_3 and TiB_2	60	60
Sharifi et al.(28)	30 nm Al_2O_3, 46 nm TiB_2	40	31.5
Khaghani-Dehaghani et al. (29)	20 nm Al_2O_3, 32 nm TiB_2	20	1.5
Rabiezadeh et al. (30)	Less than 500 nm Al_2O_3 and TiB_2	30	30

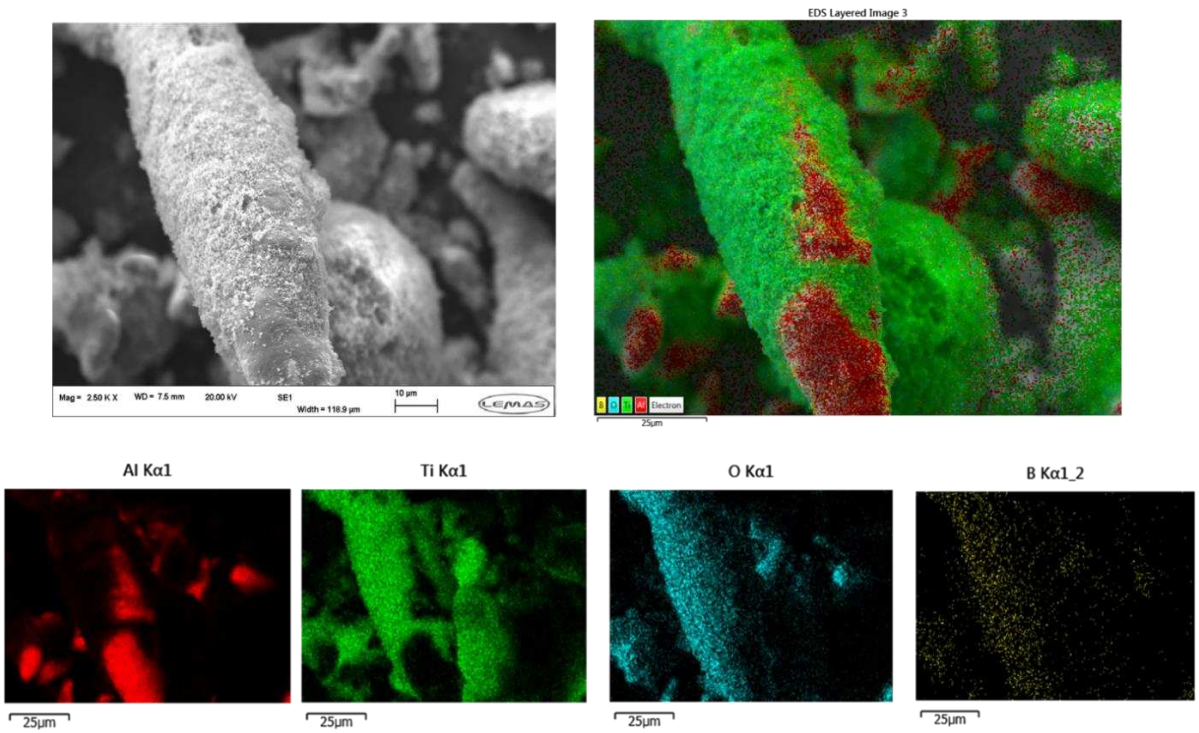

Figure 2. Al particles coated with shattered TiO2 and B2O3 particles, observed with SEM and EDS.

Thermal analysis on the milled powder, Figure 3, displays 4 endotherm peaks which correspond to water removal from the powder mixture at 120 ºC, decomposition of H_3BO_3 to B_2O_3 at 176 ºC, melting of boron at 450 ºC and melting of aluminium at 660 ºC, during the heating phase. Melting of aluminium is a result of the breaking of the thin Al_2O_3 layer coating the Al particles, due to the difference in their expansion coefficients (32, 54). Three exotherm peaks are present, at 876 ºC, 958 ºC and 1167 ºC, which correspond to alumina-thermic reduction of TiO_2 and the formation of intermediate product $AlTi_3$ (32), formation of TiB_2 (29) and formation of $Al_{18}B_4O_{33}$ from $AlTi_3$ and Al_2O_3 (32) respectively, Table 4. In literature, the exotherm at 958 ºC, for the formation of TiB_2, corresponds to the reaction of ($AlTi_3$ + 6B = 3TiB_2 + Al) (32). During the cooling phase, seems that leftover aluminium solidifies at 660 ºC.

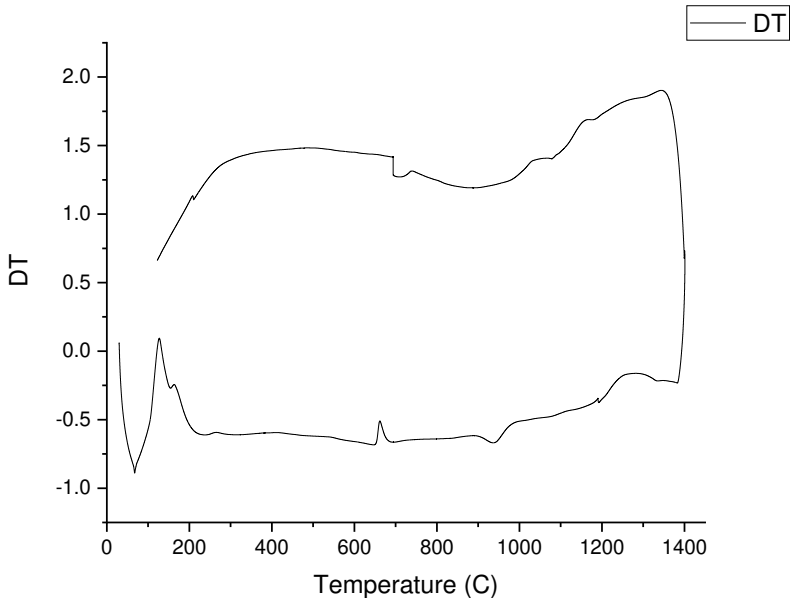

Figure 3.Thermal analysis data of the Al-TiO2-B2O3 in argon environment, with heating rate 20 C/min, up to 1400 C.

Table 4. Analysis of the peaks arising from the thermal analysis plots.

Peak Type	Temperature (°C) Reference (29)	Temperature (°C)	Reason (29, 32)
Endotherm	110	120	Water removal
Endotherm	180	176	H_3BO_3 to B_2O_3
Endotherm	-	460	Reduction of B_2O_3
Endotherm	660	660	Al melting
Exotherm	730	876	Alumino-thermic reduction of TiO_2 (TiAl3)
Exotherm	960	958	$Ti + 2B = TiB_2$
Exotherm	1134 (32)	1167	$Al_{18}B_4O_{33}$ from $AlTi_3$ and Al_2O_3
Exotherm	-	660	Al solidification (Cooling cycle)

In situ sintering of the powder mixture in a tube furnace, under inert conditions, at 1000 C for 1 hour, triggered the alumina-thermic reduction for the formation of the composite. X-Ray diffraction analysis displays 3 phases in the final composite, the ones of Al_2O_3, TiB_2 and Ti_2O_3. It is believed that the atmospheric water absorbed by B_2O_3, formed a mixture of H_3BO_3 - B_2O_3, which slightly altered the stoichiometric ratio of the milled reactants (9, 35). Eventually, abundance of TiO_2 was present, resulting in the formation of Ti_2O_3 phase in the final composite, Figure 4.

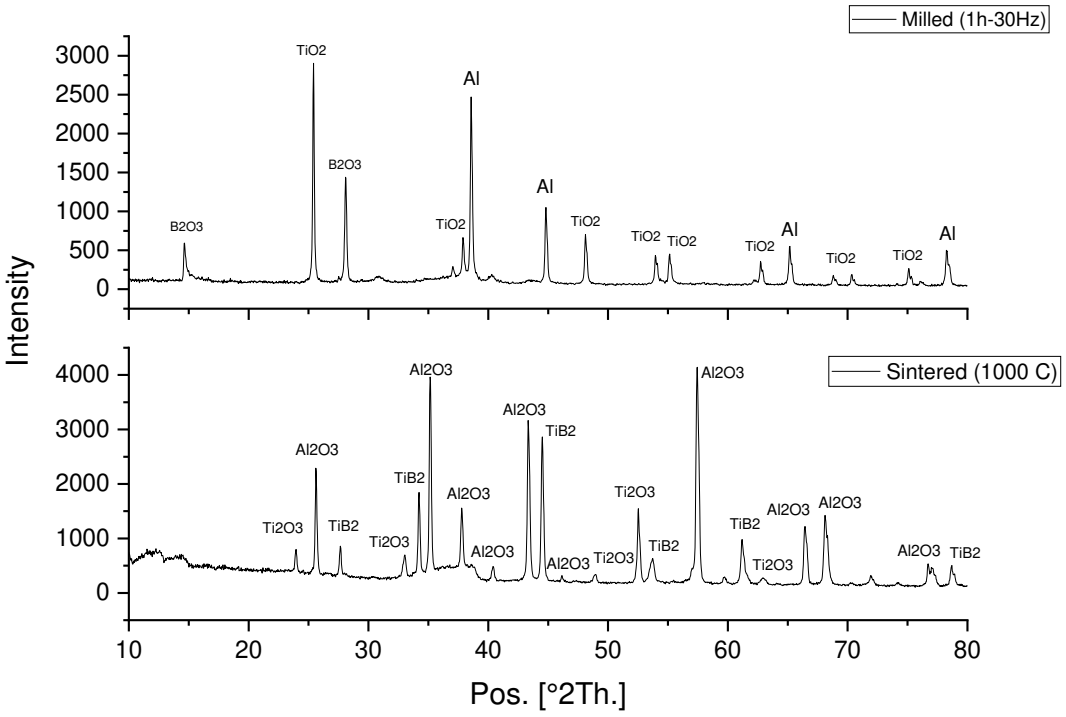

Figure 4. Phase identification of a) Un-Reacted powder mixture, b) Reacted sintered material, using X-Ray Diffraction with monochromatic CuKα radiation (λ=0.154 nm) and a 2θ range of 10–90°.

Regarding morphological aspects of the microstructure, transfer of oxygen from the oxides on the surface of aluminium particles, to aluminium, during the reaction, resulted in alumina particles formation, while free Ti and B, formed TiB_2 nano-particles on the surface of Al_2O_3, Figure 5, at approximate temperature 958 – 1000 °C. Sintering, which was a result of the highly exothermic character of reaction 1, resulted in a microstructure consisted of alumina clusters, surrounded by agglomerated clusters of TiB_2 and Ti_2O_3 nano-particles.

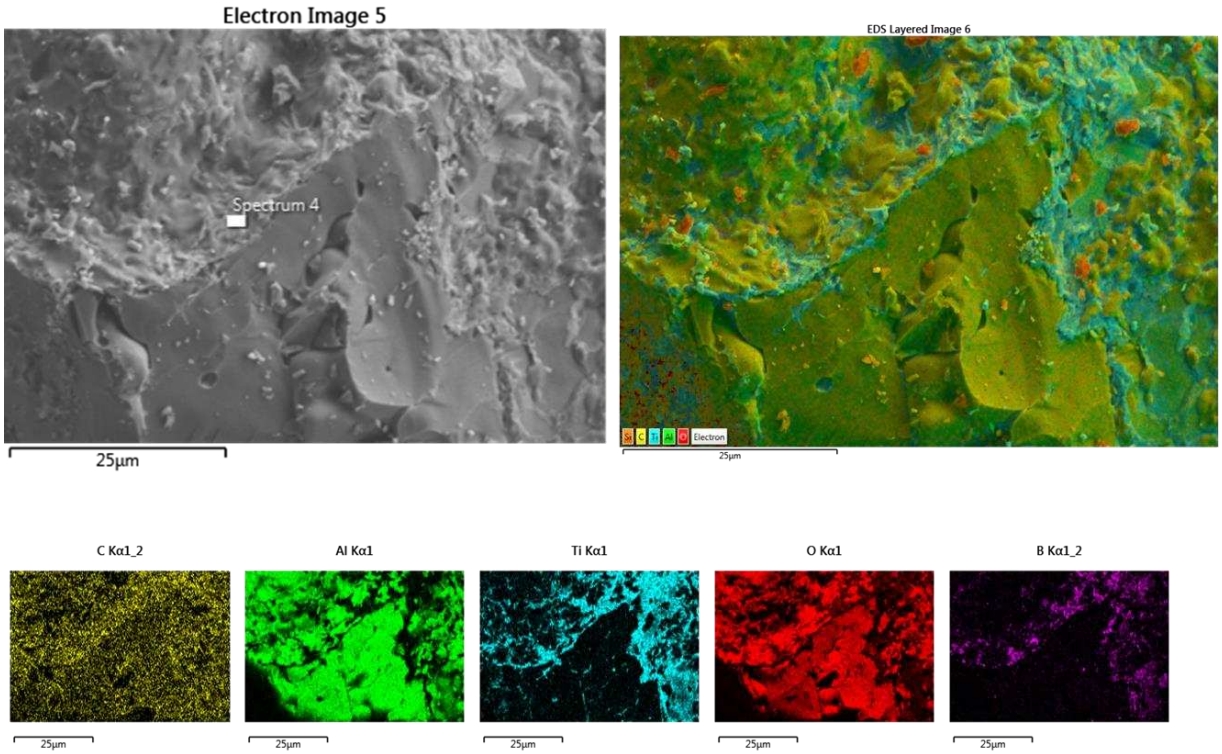

Figure 5. Al_2O_3 particles coated with TiB_2.

Conclusions

In-situ sintering of Al-TiO_2-B_2O_3 resulted in a matrix composite displaying Al_2O_3, TiB_2 and Ti_2O_3 phases, as the atmospheric water absorption by B_2O_3, altered the stoichiometric composition, allowing excess TiO_2. During sintering, the presence of moisture in B_2O_3 also increases boron loss during ignition, enabling larger concentration of Ti_2O_3 phase in the final composite. Thermal analysis data show that the reaction completes at around 958-1000 ^oC. Milled aluminium particles, coated with nano-particles of TiO_2 and B_2O_3, when heat treated at 1000 ^oC, resulted in alumina particles coated with TiB_2 and Ti_2O_3, after the completion of exothermic reaction 1.

Acknowledgements

The financial supports for this work from the DSTL office and lab facilities provided by the University of Leeds, are gratefully acknowledged.

References

1. Kingery, W.D. Introduction to ceramics. 1976.
2. Dorri Moghadam, A., Omrani, E., Lopez, H., Zhou, L., Sohn, Y. and Rohatgi, P.K. Strengthening in hybrid alumina-titanium diboride aluminum matrix composites synthesized by ultrasonic assisted reactive mechanical mixing. *Materials Science and Engineering: A.* 2017, **702**, pp.312-321.
3. Azom. Alumina - Aluminium Oxide - Al2O3 - A Refractory Ceramic Oxide. 2001. [Online]. Accesed 4 Sep 2021. Available from: https://www.azom.com/
4. Munro, R.G. Material properties of titanium diboride. *Journal of Research of the National Institute of Standards and Technology.* 2000, **105**(5), p.709.
5. Goldschmid, H.J. *Interstitial alloys.* Springer, 2013.
6. Munir, Z.A., Anselmi-Tamburini, U. and Ohyanagi, M. The effect of electric field and pressure on the synthesis and consolidation of materials: A review of the spark plasma sintering method. *Journal of Materials Science.* 2006, **41**(3), pp.763-777.
7. Palicka, R. and Rubin, J. *Development, Fabrication and Ballistic Testing of New, Novel Low-Cost High Performance Ballistic Materials.* CERCOM INC VISTA CA, 1991.

8. Wang, D. Effects of additives on combustion synthesis of Al2O3–TiB2 ceramic composite. *Journal of the European Ceramic Society.* 2009, **29**(8), pp.1485-1492.
9. Rabiezadeh, A., Ataie, A. and Hadian, A.M. Sintering of Al2O3–TiB2 nano-composite derived from milling assisted sol–gel method. *International Journal of Refractory Metals and Hard Materials.* 2012, **33**, pp.58-64.
10. Wang, W., Fu, Z., Wang, H. and Yuan, R.J.J.o.t.E.C.S. Influence of hot pressing sintering temperature and time on microstructure and mechanical properties of TiB2 ceramics. 2002, **22**(7), pp.1045-1049.
11. Liu, G., Yan, D. and Zhang, J.J.J.o.W.U.o.T.-M.S.E. Microstructure and mechanical properties of TiB 2-Al 2 O 3 composites. 2011, **26**(4), pp.696-699.
12. Goodfellow. Titanium Diboride (TiB2) - Properties and Applications. 2001. [Online]. Accesed 4 Sep 2021. Available from: https://www.azom.com/
13. Kok, M. Production and mechanical properties of Al2O3 particle-reinforced 2024 aluminium alloy composites. *Journal of Materials Processing Technology.* 2005, **161**(3), pp.381-387.
14. Königshofer, R., Fürnsinn, S., Steinkellner, P., Lengauer, W., Haas, R., Rabitsch, K. and Scheerer, M. Solid-state properties of hot-pressed TiB2 ceramics. *International Journal of Refractory Metals and Hard Materials.* 2005, **23**(4), pp.350-357.
15. Munir, Z.A. and Holt, J.B. *Combustion and plasma synthesis of high-temperature materials.* United States: VCH Publishers Inc, 1990.
16. Subrahmanyam, J. and Vijayakumar, M. Self-propagating high-temperature synthesis. *Journal of Materials Science.* 1992, **27**(23), pp.6249-6273.
17. Borovinskaya, I.P. *Ch*emical classes of the SHS processes and materials. Pure and Applied Chemistry. 1992, 64, p.919. [Accessed September 2021]. Available from: https://www.degruyter.com/
18. Mossino, P.J.C.I. Some aspects in self-propagating high-temperature synthesis. 2004, **30**(3), pp.311-332.
19. Moore, J.J. and Feng, H.J. Combustion synthesis of advanced materials: Part I. Reaction parameters. *Progress in Materials Science.* 1995, **39**(4), pp.243-273.
20. Wang, L.L., Munir, Z.A. and Maximov, Y.M. Thermite reactions: their utilization in the synthesis and processing of materials. *Journal of Materials Science.* 1993, **28**(14), pp.3693-3708.
21. Munir, Z., Anselmi-Tamburini, U. and Ohyanagi, M.J.J.o.M.S. The effect of electric field and pressure on the synthesis and consolidation of materials: A review of the spark plasma sintering method. 2006, **41**(3), pp.763-777.
22. Feng, A., Munir, Z.J.M. and B, M.T. The effect of an electric field on self-sustaining combustion synthesis: Part I. Modeling studies. 1995, **26**(3), p.581.
23. Yi, H.C. and Moore, J.J.J.o.m.S. Self-propagating high-temperature (combustion) synthesis (SHS) of powder-compacted materials. 1990, **25**(2), pp.1159-1168.
24. Feng, A., Graeve, O.A. and Munir, Z.A. Modeling solution for electric field-activated combustion synthesis. *Computational Materials Science.* 1998, **12**(2), pp.137-155.
25. Merzhanov, A.G. Problems of Combustion in Chemical Technology and in Metallurgy. *Russian Chemical Reviews.* 1976, **45**(5), pp.409-420.
26. Levashov, E.A., Mukasyan, A.S., Rogachev, A.S. and Shtansky, D.V. Self-propagating high-temperature synthesis of advanced materials and coatings. *International Materials Reviews.* 2017, **62**(4), pp.203-239.
27. Mohammad Sharifi, E., Karimzadeh, F. and Enayati, M.H. Synthesis of titanium diboride reinforced alumina matrix nanocomposite by mechanochemical reaction of Al–TiO2–B2O3. *Journal of Alloys and Compounds.* 2010, **502**(2), pp.508-512.
28. Sharifi, E.M., Karimzadeh, F. and Enayati, M.H. Preparation of Al2O3–TiB2 nanocomposite powder by mechanochemical reaction between Al, B2O3 and Ti. *Advanced Powder Technology.* 2011, **22**(4), pp.526-531.
29. Khaghani-Dehaghani, M.A., Ebrahimi-Kahrizsangi, R., Setoudeh, N. and Nasiri-Tabrizi, B. Mechanochemical synthesis of Al2O3–TiB2 nanocomposite powder from Al–TiO2–H3BO3 mixture. *International Journal of Refractory Metals and Hard Materials.* 2011, **29**(2), pp.244-249.
30. Rabiezadeh, A., Hadian, A., Ataie, A.J.I.J.o.R.M. and Materials, H. Preparation of alumina/titanium diboride nano-composite powder by milling assisted sol–gel method. 2012, **31**, pp.121-124.

31. Yang, W., Dong, S.J., Yangli, A.Z. and Xie, Z.X. Synthesis of Al2O3-TiB2 composite powder by planetary milling from Al-TiO2-B2O3-Ni mixture. In: *Applied Mechanics and Materials*: Trans Tech Publ, 2013, pp.734-737.
32. Sundaram, V., Logan, K. and Speyer, R. Aluminothermic reaction path in the synthesis of a TiB 2–Al 2 O 3 composite. *Journal of materials research.* 1997, **12**(7), pp.1681-1684.
33. Plovnick, R.H. and Richards, E.A.J.M.r.b. New combustion synthesis route to TiB2-Al2O3. 2001, **36**(7-8), pp.1487-1493.
34. Li, J., Cai, Z., Guo, H., Xu, B. and Li, L. Characteristics of porous Al2O3–TiB2 ceramics fabricated by the combustion synthesis. *Journal of Alloys and Compounds.* 2009, **479**(1), pp.803-806.
35. Kecskes, L.J., Niiler, A., Kottke, T., Logan, K.V. and Villalobos, G.R.J.J.o.t.A.C.S. Dynamic Consolidation of Combustion-Synthesized Alumina-Titanium Diboride Composite Ceramics. 1996, **79**(10), pp.2687-2695.
36. Meyers, M.A., Olevsky, E.A., Ma, J. and Jamet, M. Combustion synthesis/densification of an Al2O3–TiB2 composite. *Materials Science and Engineering: A.* 2001, **311**(1), pp.83-99.
37. Yu. Popov, A., Sivak, A.A., Yu. Borodianska, H. and Shabalin, I.L. High toughness TiB2–Al2O3 composite ceramics produced by reactive hot pressing with fusible components. *Advances in Applied Ceramics.* 2015, **114**(3), pp.178-182.
38. KURTOĞLU, A. *Aluminum Oxide and Titanium Diboride Reinforced Metal Matrix Composite and Its Mechanical Properties*. thesis, Citeseer, 2004.
39. Xu, J., Zou, B., Tao, S., Zhang, M. and Cao, X. Fabrication and properties of Al2O3–TiB2–TiC/Al metal matrix composite coatings by atmospheric plasma spraying of SHS powders. *Journal of Alloys and Compounds.* 2016, **672**, pp.251-259.
40. Chatterjee, S., Shariff, S.M., Datta Majumdar, J. and Roy Choudhury, A. Development of nano-structured Al2O3-TiB2-TiN coatings by combined SHS and laser surface alloying. *The International Journal of Advanced Manufacturing Technology.* 2008, **38**(9), pp.938-943.
41. Kimura, I., Hotta, N., Hiraoka, Y., Saito, N. and Yokota, Y. Sintering and characterization of Al2O3-TiB2 composites. *Journal of the European Ceramic Society.* 1989, **5**(1), pp.23-27.
42. Tang, W., Fu, Z., Zhang, J., Wang, W., Wang, H., Wang, Y. and Zhang, Q.J.P.t. Fabrication and characteristics of TiB2/Al2O3 core/shell particles by hybridization. 2006, **167**(3), pp.117-123.
43. Cheng, H., Li, Z. and Shi, Y.J.S.E. Microstructure and wear resistance of Al2O3–TiB2 composite coating deposited by axial plasma spraying. 2008, **24**(6), pp.452-457.
44. Eskandari, H. and Taheri, R.J.P.M.S. A novel technique for development of aluminum alloy matrix/TiB2/Al2O3 hybrid surface nanocomposite by friction stir processing. 2015, **11**, pp.503-508.
45. Sajedi Alvar, F., Heydari, M., Kazemzadeh, A., Vaezi, M. and Nikzad, L. Al2O3-TiB2 nanocomposite coating deposition on Titanium by Air Plasma Spraying. *Materials Today: Proceedings.* 2018, **5**(7, Part 3), pp.15739-15743.
46. Mousavian, R.T., Sharafi, S., Shariat, M.J.I.J.o.M.S. and Engineering. Preparation of nano-structural Al2O3-TiB2 in-situ composite using mechanically activated combustion synthesis followed byintensive milling. 2011, **8**(2), pp.1-9.
47. Reed, J.S. Principles of ceramics processing. 1995.
48. Meyers, M., Olevsky, E., Ma, J. and Jamet, M. Combustion synthesis/densification of an Al2O3–TiB2 composite. *Materials Science and Engineering: A.* 2001, **311**(1-2), pp.83-99.
49. Daněk, V. Chapter 3 - Phase Equilibria. In: Daněk, V. ed. *Physico-Chemical Analysis of Molten Electrolytes*. Amsterdam: Elsevier Science, 2006, pp.107-219.
50. Mills, A.F. *Basic heat and mass transfer.* Prentice hall, 1999.
51. Chauruka, S.R., Hassanpour, A., Brydson, R., Roberts, K.J., Ghadiri, M. and Stitt, H. Effect of mill type on the size reduction and phase transformation of gamma alumina. *Chemical Engineering Science.* 2015, **134**, pp.774-783.
52. Seetharaman, S. *Fundamentals of metallurgy.* Taylor & Francis, 2005.
53. Mohammad Sharifi, E., Karimzadeh, F. and Enayati, M.H. Mechanochemically synthesized Al2O3–TiC nanocomposite. *Journal of Alloys and Compounds.* 2010, **491**(1), pp.411-415.
54. Logan, K., Sparrow, J. and McLemore, W. Experimental modeling of particle-particle interactions during SHS of TiB 2-Al 2 O 3. In: *Combustion and plasma synthesis of high-temperature materials*. 1990.